# CONTROL AND TOPOLOGICAL OPTIMIZATION OF A LARGE MULTIBEAM ARRAY ANTENNA

Thierry Touya and Didier Auroux
Mathematics Institute of Toulouse
University of Toulouse *Paul Sabatier*
31062 Toulouse cedex 9
France
email: {touya;auroux}@mip.ups-tlse.fr

**ABSTRACT**
We consider Direct Radiating Arrays (DRA) as reconfigurable multibeam transmit antennas. The antenna diameter is determined by directivity and isolation specifications, and the grid lattice is constrained by grating lobe rejection outside the Earth. As high directivity beams are mostly required, adding these two constraints leads to a prohibitive number of antenna elements (so of active chains).

In order to reduce the number of active chains without affecting antenna pattern characteristics, we consider non regular aperture sampling by dividing the radiating aperture into non-regular subarrays. Industrial constraints lead to gather small identical elements in rectangular groups with various sizes. The basic elements are small enough to avoid any grating lobe on the Earth disk; as the 2nd-step aperture meshing (by non-regular groups) is non-periodic, no other grating lobes appear on the Earth.

We first present a mathematical algorithm for the optimization of the antenna alimentation for a given spot on the Earth, by defining a cost function able to warrant convergence of a gradient-type method, and then we combine these solutions found for each beam in a single power distribution on the aperture, using the Singular Value Decomposition (SVD) method. Finally, we optimize the topology of the antenna by sampling the obtained distribution into amplitude values that can be provided by gathering elements by 1, 2, 3, or 4. And the best rectangles arrangement is found in an iterative process using the topologic gradient method.

A clever association of these various steps leads to a non-regular subarrays distribution saving nearly $50\%$ of the initial elements number, while complying for all beams with typical requirements on gain and isolation, and using equal-power feeding, so better efficiency and lower cost for a single amplifiers class.

**KEY WORDS**
Array antenna, multi-beam, topological optimization, active chain reduction.

## 1 Introduction

Some recent missions of geostationary satellites require a large number of beams with high directivity, for example fast internet access from/to anywhere, especially in the zones not covered by wired ADSL, and broadcasting high-definition TV programs dedicated to specific linguistic zones. Well suited transmit antennas are Active Arrays (operating in Ku-band around 12GHz or Ka-band around 20GHz). But a high directivity needs a large antenna diameter (1 to 2m for 0.6 to $1^o$ beams; depending on Ku or K band), and covering a significant Earth zone means a $6^o$ to $8^o$ angular domain as seen from the satellite. Another constraint for these geostationary satellites is to reject out of all terrestrial regions the array grating lobes, in order to comply with frequency spectrum re-use among several systems.

The latter conditions require several hundreds of radiating elements and associated active chains, when using classical designs with periodic regular array lattice. This number much exceeds that of phase-control points required to shape and point the antenna pattern(s). Furthermore, this implies a complex Beam Forming Network (analogue or digital). The cost of such an antenna is prohibitive. The idea is then to reduce drastically the number of parallel RF paths in such large multibeam active arrays. This problem has already been studied, for example by considering thinned arrays or non-regular sub-arraying (see e.g. [2]).

Using some optimization tools, we present a global algorithm for such reduction, without any loss in the global performance of the antenna. In section 2, we define our generic test-case, with the various directivity constraints on the different zones of the Earth. Then, we present in section 3 an optimization algorithm for the computation of optimal feeding laws, by defining a convex cost-function to be minimized. Using some data reduction technique (Singular Value Decomposition method), we show in section 4 that all the optimal feeding laws found for each beam have almost the same feeding power. This allows us to optimize the geometry of the antenna by gathering radiating elements, accordingly to this law. We finally validate our non-regular subarrays distribution in section 5.

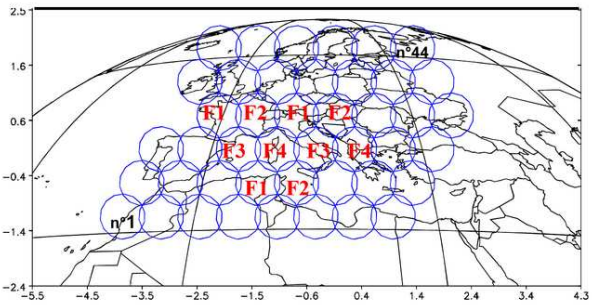


Figure 1. Test-case coverage by $44$ beams with $0.8^o$ diameter.

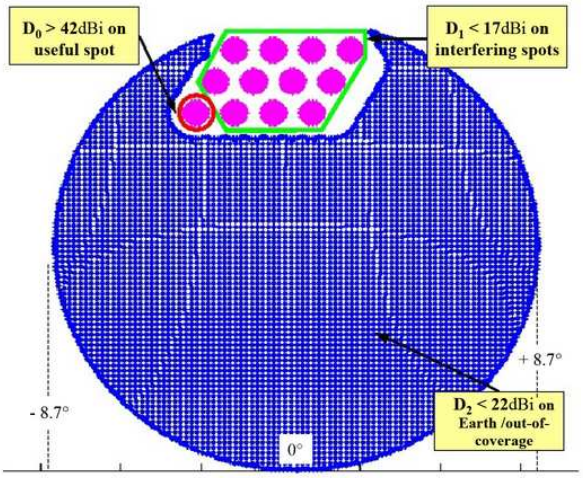


Figure 2. Definition of the various zones, restricting to the pink spots using the same sub-band: useful spot (UTI zone, in red), interfering spots (INT zone, in green) and Earth outside the UTI and INT zones (in blue).

## 2 Generic test-case

We consider a generic multi-beam coverage, with 44 beams with $0.8^o$ diameter, and a 4-subband frequency re-use in the same band (see figure 1, and e.g. [2] for more details about this kind of generic test-case).

The main requirements concerning antenna beams are illustrated (also in a generic way) in figure 2, and the directivity constraints for our test-case are the following:

- Directivity over the useful spot $D_0$ (UT1 zone): $> 42$ dBi;
- Directivity over the interfering spots $D_1$ (INT zone): $< 17$ dBi;
- Directivity over Earth, out of the coverage $D_2$ (ISO zone): $< 22$ dBi.

The antenna is made of $n$ feeds (each connected to an active path including a specific phase-control for each beam), and we denote by $a_i$ the complex excitation of feed $i$. The several constraints on the array antenna *complex excitations* vector $a = (a_i)_{i=1...n}$ and the radiated power over the various zones defined in figure 2 are:

- $|a_i|^2 = \frac{1}{n}$ for all radiating elements, as all feeds shall radiate the same power (we normalise the total antenna power is equal to 1);
- $|E(a,x)|^2 \geq g_0$ for all points $x$ in the covered spot, in order to comply with the minimal directivity requirement;
- $|E(a,x)|^2 \leq g_1$ for all points $x$ in the other spots, in order to minimize interferences in the same sub-band;
- $|E(a,x)|^2 \leq g_2$ for all points $x$ in the isolation zone, i.e. on the Earth, outside the UTI and INT zones.

## 3 Optimization of the alimentations

### 3.1 Constraints modification

As the final goal is to reduce the number of antenna feeds by gathering some radiating elements, the idea is to relax the first constraint on the excitation power, and to gather feeds with small excitation modulus. The non-convex first constraint is then replaced by a convex constraint:

$$|a_i|^2 \leq \frac{1}{n}, \quad \text{for all radiating elements.} \tag{1}$$

The radiated power $|E(a,x)|^2$ is a (quadratic) convex function of the excitation vector $a = (a_i)$, and all the constraints are now convex, except the second one. So we replace this inequality by an equality constraint (which is convex); instead of maximizing the energy inside the spot coverage, the electrical field should be equal to a given value at the centre of the spot:

$$E(a, x_0) = g_0 + \delta_0, \tag{2}$$

where $x_0$ is the centre of the desired spot, and $\delta_0$ a parameter to be tuned.

This will ensure that the radiated power is greater than $g_0$ if $\delta_0$ is large enough. This works because the solid angle of the spot is small.

Usually, the alimentation $a$ solution to the original problem is defined up to a constant phase change. Thanks to the last modification, the phase is fixed by imposing $g_0 + \delta_0$ to be a real number. By reducing the set of possible solutions, we improve the quality of our optimization problem.

Notice that we don't use decibels for aperture field and radiating one evaluation, because it destroys the so important quadratic property of the power, appearing in most constraining equations.

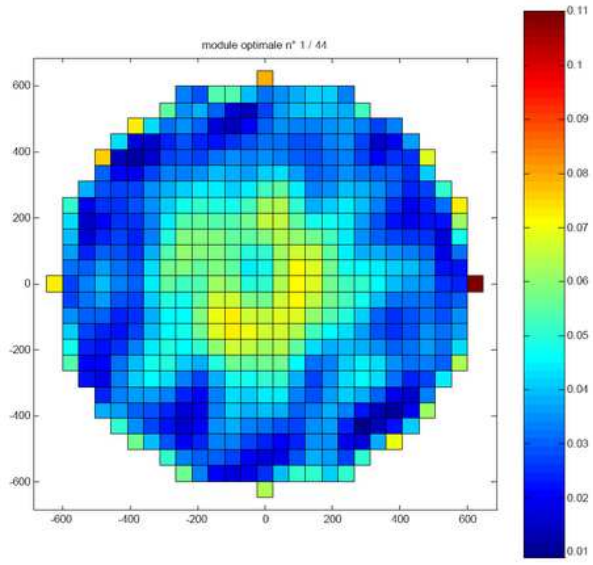


Figure 3. Optimized excitation amplitudes for spot 1.

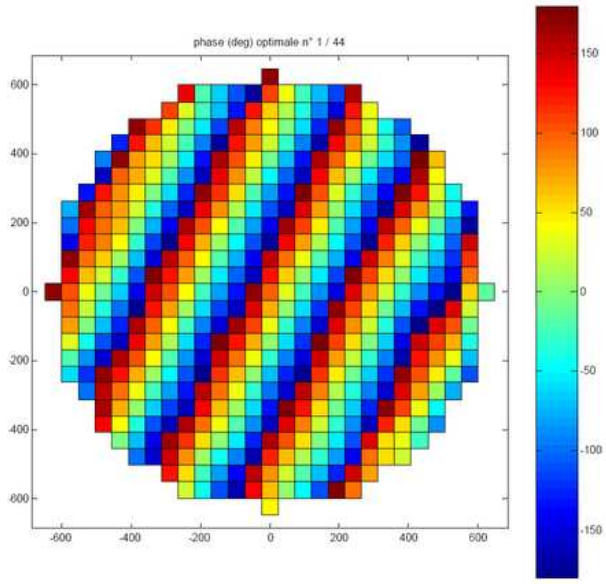


Figure 4. Optimized excitation phases for spot 1.

All the constraints are now convex: we are sure to reach an optimal solution using a descent method, without being trapped in a local minimum.

### 3.2 Cost function and minimization

In order to find an excitation vector satisfying all these constraints, we define a vector function F, in which each component is related to the compliance with one of these constraints (the component is null if and only if the constraint is satisfied). We finally define the following cost function

$$J(a) = \frac{1}{2}\|(F(a))^+\|^2, \tag{3}$$

where $X^+$ means *positive part of a real number X*.

The excitation vector satisfies all constraints if and only if $J(a) = 0$. The idea is then to minimize the functional $J$ with respect to the real and imaginary parts of $a$, and not to the modulus and phase for linearity purpose. This unconstrained minimization is performed with a Levenberg-Marquardt algorithm [3], and provides an optimal excitation vector a for each spot.

### 3.3 Numerical experiments

Figure 3 shows for the first spot the optimal excitation amplitudes of all radiating elements, and figure 4 shows the optimal excitation phases for the same spot. We can see that the amplitude is high in the middle of the antenna and much weaker on the side. The optimal phases clearly show the signal dephasing, in order to concentrate the energy on the bottom-left spot (see figure 1).

## 4 Topological optimization of the antenna

### 4.1 Singular value decomposition

We have seen in the previous section how to find an optimal excitation vector $a$ for each spot on the Earth. If we denote by $s$ the number of spots, we can define a $n \times s$ matrix $A$, in which the $k^{\text{th}}$ column ($1 \leq k \leq s$) contains the modulus of the optimal excitation vector $a$ corresponding to spot $k$, provided by the previous minimization with the convex inequality constraint on the modulus of $a$.

In order to easily extract the maximum of information from all these excitations, we will apply the Singular Value Decomposition (SVD) method to this matrix [1]. The main result of this theory states that the matrix $A$ has a factorization of the form

$$A = U\Sigma V^*, \tag{4}$$

where $U$ is a $n \times n$ unitary matrix (i.e. $UU^* = U^*U = I$, identity matrix), $V$ is a $s \times s$ unitary matrix, $V^*$ is the conjugate transpose of $V$, and $\Sigma$ is a $n \times s$ real matrix with non-negative numbers on the diagonal and zeros off the diagonal. The $\Sigma$ matrix contains the singular values $(\sigma_i)$ of $A$, which can be thought of as scalar *gain controls* by which each corresponding input is multiplied to give a corresponding output. A common convention is to arrange the singular values in decreasing order. In this case, the diagonal matrix $\Sigma$ is uniquely determined.

Some practical applications need to solve the problem of approximating a matrix $A$ with another matrix $\tilde{A}$ which has a smaller rank $r$. In the case where this is based on minimizing the Frobenius norm of the difference between $A$ and $\tilde{A}$ under the constraint that $rank(\tilde{A}) = r$, it turns

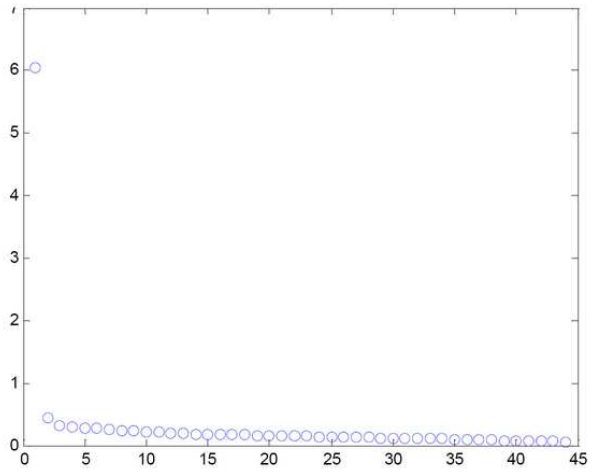


Figure 5. Singular value decomposition (SVD) of optimal excitations matrix.

out that the solution is given by the SVD of $A$, namely

$$\tilde{A} = U\Sigma' V^*, \tag{5}$$

where $\Sigma'$ is the same matrix as $\Sigma$ except that it contains only the $r$ largest singular values (the other singular values are replaced by zero). The Frobenius square norm of the difference between $A$ and $\tilde{A}$ is the sum of the square singular values that have not been kept:

$$\sigma_{r+1}^2 + \sigma_{r+2}^2 + \ldots + \sigma_s^2, \tag{6}$$

and decreases when $r$ is increased.

Usually, in most applications (as shown on figure 5, for the present text-case described in the previous sections), the decrease of the singular values is such that the greatest one $\sigma_1$ is much larger than the others, and they quickly decrease to 0. If one only keeps the first singular value (i.e. the rank of $\tilde{A}$ is $r = 1$), the approximation is still very accurate and becomes

$$\tilde{A} = \sigma_1 u_1 v_1^*, \tag{7}$$

where $u_1$ is the first column of $U$ and $v_1^*$ is the first row of $V^*$. Then, the most part of the information contained in $A$ can be expressed with only $u_1$. In other words, all modulus of the $s$ excitation vectors are proportional to the vector $u_1$. We have finally reduced $s$ excitation vectors to only one, represented in figure 6.

### 4.2 Optimization algorithm

Some neighbouring feeds will be merged in order to minimize the number of antenna feeds and hence of phase control points. In such case, the number n of radiating elements will decrease, and as the total power does not change, the constraints on each feed modulus will change. For example, if we merge 2 feeds, we have the following configuration change:

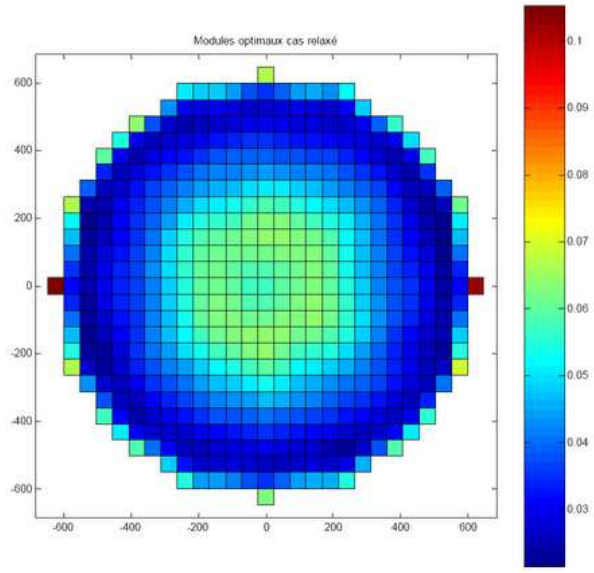


Figure 6. Optimum amplitudes for all spots provided by the SVD.

- before gathering in $n$ feeds, with $|a_i|^2 = \dfrac{1}{n}$;
- after merging: $n-1$ feeds, with $|a_i|^2 = \dfrac{1}{n-1}$ for all feeds, except for the two merged ones: $|a_i|^2 = \dfrac{0.5}{n-1}$.

In case some neighbouring feeds have comparable excitation modulus, they will be merged according to several predefined geometries. In the following, we will only consider only merging of 2, 3 or 4 feeds together, according to a rectangular contour (which includes the square cases: $1 \times 1$ or $2 \times 2$ initial R.E.).

For a given antenna with $n$ radiating elements, we denote for each radiating element $i$ by

- $r_i$, $1 \leq r_i \leq 4$, the number of R.E. possibly merged into the feed to which the concerned R.E. belongs;
- $c_i^n = \dfrac{1}{\sqrt{r_i n}}$ the theoretical excitation modulus imposed by the constraint of fixed total power, equally shared among all groups;
- $m_i$ the $i^{\text{th}}$ component of the first vector $u_1$ of the singular value decomposition of the excitation matrix $A$ (see previous subsections).

We can now define a cost function measuring the difference between the theoretical and computed excitation modulus:

$$I_k = \sum_{i=1}^{n} (c_i^n - m_i)^2, \tag{8}$$

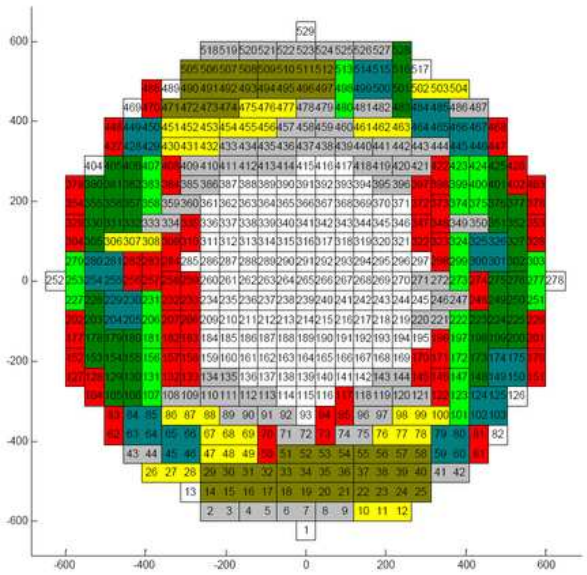

Figure 7. Optimized geometry of the antenna.

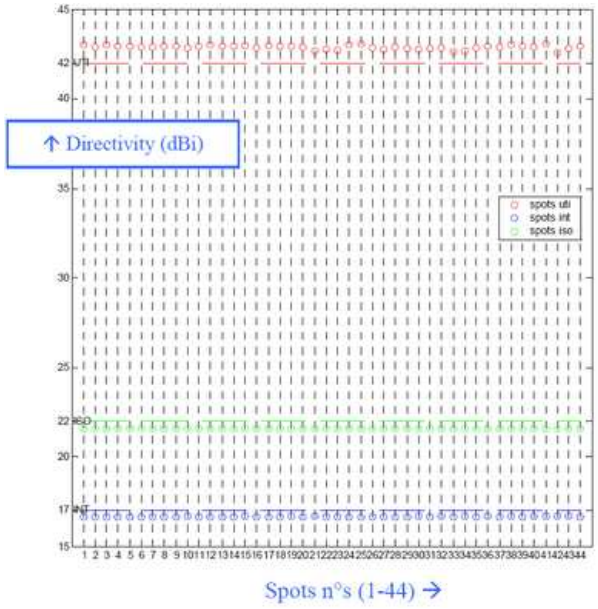


Figure 8. Fully compliant performances of the final antenna.

where $k$ suffix is the concerned iteration number. Be careful that this *cost function* is different from the initial one $J$, which led to optimized excitations separately for each spot.

The geometry of the antenna is optimized by minimizing $I_k$ at each iteration:

- find the radiating element $i_0$ maximizing the error $(c_i^n - m_i)$;
- gather all possible feeds involving this element, according to the predefined geometries, consider these few new geometries and find the one minimizing the error between the theoretical and computed excitation modulus;
- if this error is smaller than $I_k$, then validate the corresponding gathering, and set $k = k + 1$; otherwise stop (i.e. the algorithm has converged).

Figure 7 shows the optimal geometry of the antenna provided by this algorithm. The final number of radiating elements is 283, while the initial number was 529.

## 5 Global algorithm and numerical validation

As a global validation, we have to check then that the optimized array geometry complies with all initial criteria $(g_0, g_1, g_2)$.

We now sum-up here-under the mathematical procedure described in the previous sections, and illustrate with intermediate results for the antenna requirements given in section 2 as follows:

- the excitation vector $a$ is optimized with continuous possible amplitudes (alias $|a_i|$ modula), and separately (with a different solution) for each spot;
- the best *average* $\hat{a}$ (for all spots) was found thanks to the SVD, and keeping only the highest singular value. It is still a vector with *continuous* excitations modulus;
- we find the best geometrical gathering to fit the excitation modula with the *quantified* values ($|a_i|^2 = \dfrac{1}{r_i n}$) best-approaching.

With these optimized geometry and alimentation law, we compute all the array performances. As it can be seen in figure 8, they are all compliant with requirements, and even with some margin on the 3 specifications:

- UTI (minimum directivity on the concerned spot: red circle in figure 8): we are between $0.5$ and $1$ dBi below the minimum directivity on all spots;
- INT (maximum directivity on the interfering spots: blue circles): we are nearly $0.5$ dB below the maximum directivity;
- ISO (maximum directivity on the Earth, out of the coverage: green circles): here also, we are $0.5$ dB below the constraint.

We can then clearly see that the proposed geometry of the antenna complies quite easily with all the initial constraints, with only $283$ radiating elements (instead of $529$ in the initial geometry).

## 6 Conclusion

We assessed several optimization algorithms for reducing the number of phase-control points in large arrays with multiple beams. The main conclusions are the following. By rewritting in a well-chosen way the alimentation law optimization problem, we obtained an efficient algorithm for chosing the alimentations. Then, the use of the singular value decomposition method, coupled with a geometrical optimization algorithm, appeared compulsory to reach safely solutions for elements gathering, with all beams compliant with the chosen typical requirements: up to $50\%$ number of phase-control have been saved in a non-regular array comprising only 4 kinds of rectangular subarrays. This induces a low cost increase, compared to the large one coming from decreasing the number of active chains. This method present also another advantage for industrial implementation: the taper which is compulsory for low side-lobes is provided by the non-regular density of elements feeding points. So in a transmit antenna, all amplifiers would provide the same power, working at the same well-optimized operating point. We may also consider some more kinds of subarrays (not only from $1 \times 1$ to $1 \times 4$) in order to reduce again the number of active chains.

## References


[1] G. H. Golub and C. F. Van Loan, *Matrix Computations* (Johns Hopkins University Press, Baltimore, 1996).

[2] C. Guiraud, Y. Cailloce and G. Caille, Reducing direct radiating array complexity by thinning and splitting into non-regular subarrays, *Proc. 29th ESA Antenna Workshop*, Noordwijk, The Netherlands, 2007.

[3] D. Marquardt, An algorithm for least-squares estimation of nonlinear parameters, *SIAM J. Appl. Math.*, 11, 1963, 431-441.